Supplement of Biogeosciences, 15, 4973–4993, 2018
https://doi.org/10.5194/bg-15-4973-2018-supplement

Biogeosciences Open Access EGU

Supplement of

Mechanisms of dissolved and labile particulate iron supply to shelf waters and phytoplankton blooms off South Georgia, Southern Ocean

Christian Schlosser et al.

Correspondence to: Christian Schlosser (cschlosser@geomar.de)

Supplementary Text

Text S1: Seawater sampling and analysis

Water column samples were collected using trace metal clean OTE bottles deployed on a Kevlar line. The OTE bottles were transferred into the clean container where all sample handling was performed. Dissolved and total dissolvable seawater samples were acidified immediately with concentrated trace metal grade nitric acid (HNO_3, UpA, Romil) to pH 1.66 (22 mmol H^+ L^{-1}). Acidified seawater samples were shipped to the National Oceanography Centre Southampton and analyzed by isotope dilution (ID) and standard addition inductively coupled plasma - mass spectrometry (ICP-MS).

The preconcentration and ICP-MS analysis was adapted from the method outlined by Rapp et al. (2017). Approximately one year after collection, 12 mL of acidified seawater was transferred into 30 mL fluorinated ethylene propylene (FEP) bottles and spiked with a spike solution containing mainly the artificially enriched isotope of iron (^{57}Fe). For the analysis of Al, and Mn a series of four standard additions were performed on every tenth sample. To obtain equimolar conditions between the spike and the natural seawater concentration, larger amounts of spike was added to the total dissolvable seawater samples. All samples were irradiated with strong ultraviolet light for 3.5 hours. Subsequently, the sample solution was buffered to pH 6.4 using a 2 M ammonium acetate solution (pH9.2, Fisher Optima grade ammonia and acetic acid, glacial). Immediately after buffer addition the solution was preconcentrated using an automated system (Preplab, PS Analytical) that was equipped with a metal chelating resin (WACO) resin (Kagaya et al., 2009). Any remaining seawater salts were rinsed off using deionized water (> 18 MΩ cm, MilliQ, Millipore). The metals retained on the resin were eluted using 1 mL of a 1 M sub-boiled HNO_3 solution, which was collected in acid cleaned 4 mL polypropylene vials. The collected vials were placed into the auto-sampler of the ICP-MS (Element XR, Thermo).

The difference between the total dissolvable (TDM) and dissolved metal (DM) concentrations was used to determine the particulate concentration ($LP_{UN}M$ = TDM – DM). It should be noted that this particulate fraction represents the amount of Fe ($LP_{UN}Fe$), Al ($LP_{UN}Al$), and Mn ($LP_{UN}Mn$) re-dissolved from particles within 1 year after the addition of 22 mmol H^+ L^{-1}. This means acid-inert minerals (e.g. zircon) and their associated trace metals likely did not contribute to the particulate metal concentration.

Certified seawater standards (SAFe D2 and GEOTRACES D) were preconcentrated and analyzed with each batch of samples, in order to validate our sample concentration. Values obtained by us for the certified seawater standards agreed with reported values for the GEOTRACES and the SAFe standard seawater (SAFe D2: 0.92 ± 0.02 nmol Fe L^{-1} (certified 0.90 ± 0.02 nmol Fe L^{-1}), GEOTRACES D: 1.00 ± 0.04 nmol Fe L^{-1} (certified 0.95 ± 0.05 nmol Fe L^{-1}). The precision for replicate analyses was between 1-3%. The buffer blank was 0.056 ± 0.016(σ_{bl}) nmol Fe L^{-1}, and the limit of detection (3 x standard deviation of the blank) was determined as 0.061 ± 0.020(σ_{bl}) nmol Fe L^{-1}.

Certified reference materials (crm), NIST 1573a and Tort 2, were digested and analysed with each batch of suspended particle and faecal pellet samples, in order to validate our sample concentration. Values obtained agreed with reported values of the crm (NIST 1573a: 423 ± 5 mg Fe kg^{-1} (certified 368 ± 7 mg Fe kg^{-1}), 244 ± 2 mg Mn kg^{-1} (certified 246 ± 8 mg Mn kg^{-1}), 550 ± 1 mg Al kg^{-1} (certified 598 ± 12 mg Al kg^{-1}); Tort-2: 117 ± 2 mg Fe kg^{-1} (certified 105 ± 13 mg Fe kg^{-1}), 13 ± 1 mg Mn kg^{-1} (certified 14 ± 1 mg Mn kg^{-1})).

Text S2: Sediment and porewater sampling and analysis

Sediment cores with an undisturbed sediment-seawater interface were immediately transferred to a N_2-filled glove bag in a temperature-controlled laboratory to simulate ambient bottom water temperatures (approximately 4°C). Sediments were manually extruded at depth intervals of 1 or 2 cm into a polycarbonate ring, and sectioned using a polytetrafluoroethylene

(PTFE) sheet that was cleaned with deionised water between each application. Porewater was separated from each sediment section by centrifugation at 9,000 g at 4°C under N_2 for 10 minutes; the supernatant porewaters were filtered under N_2 through 0.2 μm cellulose nitrate syringe filters (Whatman, UK). Aliquots of each porewater sample were collected in acid-cleaned LDPE bottles (Nalgene) and acidified to pH <2 by adding 2 μL of concentrated hydrochloric acid (HCl, UpA, Romil) per 1 mL of sample; acidified samples were stored refrigerated prior to analysis at NOCS. Conjugate sediments were freeze dried on board and stored at room temperature, pending analysis at the NOCS.

Sub-samples (~100 mg) of the bulk, homogenized sediments were completely dissolved using hot aqua regia (HNO_3+HCl) followed by hot hydrofluoric-perchloric acid (HF-$HClO_4$) mixtures and finally diluted in 0.6M HCl as described elsewhere (Homoky et al., 2011) . The acid digests were analysed by ICP-OES (Perkin Elmer Optima 4300DV). Calibration standards were matrix-matched and blank and instrument drift were monitored and corrected for by including calibration blanks and multi-element standards with each batch of 10 analyses. To ascertain the accuracy of the method certified reference material MAG-1 (United Sates Geological Survey) was analysed with each batch of samples. The values measured in our laboratory are in close agreement with the certified values: 42.978 ± 3.155 g Fe kg^{-1} (certified 47.600 ± 4.200 g Fe kg^{-1}); 715 ± 9 ng Mn g^{-1} (certified 760 ± 69 μg Mn kg^{-1}); and 76.605 ± 2.740 g Al kg^{-1} (certified 86.800 ± 1.600 g Al kg^{-1}).

Acidified porewater samples were analysed for a suite of major and trace elements, by ICP-OES (Perkin Elmer Optima 4300 DV). Elements including Fe and Mn were measured at 50-fold dilutions of the porewater sample in 0.6M HCl. Calibration standards were matrix matched and blank and instrument drift were monitored and corrected for by including calibration blanks and multi-element standards for each batch of ten analyses. The instrument

limits of detection (LD, 3 x standard deviation of acid blanks) were 1.25 µg Fe kg^{-1} and 0.08 µg Mn kg^{-1}.

Text S3: Calculation of dissolved Fe and Mn fluxes from shelf sediment porewaters

The calculation of pore water Fe and Mn fluxes follows the approach of Boudreux and Scott (1978), who described the flux of pore water Mn(II) by diffusion and reaction through an oxygenated surface layer in marine sediments.

$$J = \frac{\varphi(D_s k_1)^{0.5} C_p}{sinh((k_1/D_s)^{0.5} L)}$$

Where J is the flux (g cm^{-2} s^{-1}) of Mn(II) from sediment pore water to bottom water, L is the thickness (cm) of the oxygenated surface layer where Mn(II) is removed from the pore water by oxidative precipitation in the sediment, and C_p is the concentration (g cm^{-3}) of Mn(II) in the pore water beneath L relative to the overlying bottom water. The diffusive rate constant, D_s (cm^2 s^{-1}), is derived from sediment porosity (φ), and the Mn(II) oxidation rate constant, k_1 (s^{-1}), is estimated from field studies (Boudreux and Scott, 1978). This method has more recently been adopted for the determination of pore water Fe(II) fluxes (Homoky et al., 2013; Raiswell and Anderson, 2005) using the Fe(II) oxidation kinetics of (Millero et al., 1987) to derive k_1, and has been favourably compared with incubated flux determinations from shelf sediments (Homoky et al., 2012).

We use measured and estimated values for scalar terms for the flux calculations that are summarised in Supplementary Table S1 to investigate the potential for pore water fluxes of Fe and Mn from sites S1, S2 and S3. Sediment porosity (φ) was measured by the change in wet sediment mass after drying sliced core samples. Oxygen penetration depth (L) was measured from a single sediment core from site S3 with a Unisense microsensor apparatus following Homoky et al. (2013), and in the absence of multiple determinations is extrapolated to each core site. Diffusion coefficients (D_S) are a derived from measurements of φ after Boudreau and Scoot (1978). The oxidation rate constant (k_1) for Mn(II) is also derived from

Boudreau and Scoot (1978). For Fe(II), k_1 is calculated from values of bottom water O_2, temperature (0 °C), salinity (34) and an estimated pore water pH of 7.5 (Homoky et al., 2012), following Millero et al. (1987) (Homoky et al., 2013; Homoky et al., 2012; Raiswell and Anderson, 2005). Values of C_P are for measured data (at 0.5 and 1.5 cm depth) closest to the depth of L from each core site. Corresponding fluxes of pore water Fe (<0.1 to 44.4 μmol m^2 d^{-1}) and Mn (0.6 to 4.1 μmol m^2 d^{-1}) fall within the range of fluxes measured from continental margin sediments of the northeast Pacific (John et al., 2012; McManus et al., 2012) and demonstrate South Georgia shelf sediments are also likely to be an important source of Fe and Mn to the water column.

Text S4: Estimation of phytoplankton Fe requirements and Fe fluxes

The Fe requirements of the phytoplankton community within the bloom were estimated by combining satellite derived marine net primary productivity data (NPP = 62 ± 21 mmol C m^{-2} d^{-1} (Ma et al., 2014)) with an average intracellular Fe:C ratio (5.2 ± 2.8 μmol Fe mol^{-1} C^{-1} (Strzepek et al., 2011)). NPP was estimated from satellite-derived information using a phytoplankton pigment absorption based model (Ma et al., 2014). The applied NPP rate corresponded to an average chlorophyll a content in the euphotic zone of ~ 4 ug L^{-1}. There are several literature values for Fe:C ratio estimates ranging from 6 – 14 μmol Fe mol^{-1} C^{-1} under natural non Fe-fertilized and 10 – 40 μmol Fe mol^{-1} C^{-1} under Fe-fertilized conditions for Southern Ocean diatoms, autotrophic flagellates, and heterotrophic flagellates (Twining et al., 2004). Lab based incubation experiments using coastal phytoplankton species, such as *Dunaliella tertiolecta, Pyramimonas parkeae, Nannochloris atomus, Pycnococcus provasoli, Tetraselmis* sp., *Gymnodinium chlorophorum, Prorocentrum mimimum, Amphidinium carterae, Thoracosphaera heimii, Emiliania huxleyia, Gephyrocapsa oceanica, Ditylum brightwellii, Thalassiosira weissflogii, Nitzschia brevirostris,*and *Thalassiosira eccentric*, reviled an average value of ~ 51 μmol Fe mol^{-1} C^{-1} (Ho et al., 2003), while Southern Ocean

phytoplankton species including *Phaeocystis antarctica* (clone AA1), *Fragilariopsis kerguelensis, Thalassiosira Antarctica*, *Eucampia Antarctica*, and *Proboscia inermis* were an order of magnitude lower between 1.8 – 8.6 (Strzepek et al., 2011). Because most phytoplankton species from the Southern Ocean are very well adapted to the very low Fe water content, we decided to apply the low Fe:C ratios provided by Strzepek et al. (Strzepek et al., 2011). The Fe:C ratio in the blooming region is presumingly higher, thus the rather low Fe:C ratio used refelcts the minimum amount of DFe that has to be supplied.

The vertical Fe flux (J_z) was calculated using an approach outlined in de Jong et al. (2012). The vertical DFe flux is the sum of advective Ekman pumping (left term) and diffusion (right term).

$$J_z = w[DFe]_{BWL} + K_z\left(\frac{\delta[DFe]}{\delta z}\right)$$

The advective Fe flux term (left) expressed by the upwelling velocity (w), which was set constant ~$1.1 * 10^{-6}$ m s^{-1} (de Jong et al., 2012), and the average dissolved Fe concentration ($[DFe]_{BWL}$) at all stations at ~ 200 m depth, contributed to 38% to the entire vertical Fe flux of 0.41 µmol m^{-2} d^{-1}. The remaining 62% are contribution of the diffusive mixing term (right term) which was derived from the DFe gradient at all stations between the surface mixed layer and ~ 200 m water depth and the vertical diffusivity, set constant at $K_z = 1 * 10^{-4}\ m^{-2}\ s^{-1}$.

Supplementary Tables

Table S1: Summary of pore water Fe and Mn flux parameters

Parameter	Unit	Fe			Mn		
Site		S1	S2	S3	S1	S2	S3
Pore w. conc. C_p	(g cm^{-3})	1.7E-07 to 9.6E-07	6.2E-08 to 8.6E-08	9.2E-08 to 1.7E-06	4.9E-08 to 1.3E-07	1.8E-08 to 4.0E-08	2.2E-08 to 2.8E-08
O_2 depth, L	(cm)	0.7	0.7	0.7	0.7	0.7	0.7
Porosity, φ		0.76	0.76	0.84	0.76	0.76	0.84
Diff. coef., D_s	(cm^2 s^{-1})	2.076E-06	2.076E-06	2.461E-06	1.877E-06	1.877E-06	2.156E-06
Bottom water [O_2]	(g cm^{-3})	1.574E-05	1.574E-05	1.700E-05	1.00E-07	1.00E-07	1.00E-07
Pore water pH		7.5	7.5	7.5	7.5	7.5	7.5
Oxidation rate, k_1	(s^{-1})	1.574E-05	1.574E-05	1.700E-05	1.00E-07	1.00E-07	1.00E-07
Flux, J	(g cm^3 s^{-1})	2.2E-13 to 1.2E-12	4.3E-15 to 6.1E-15	1.6E-13 to 2.9E-12	1.0E-13 to 2.6E-13	3.6E-14 to 8.1E-14	5.8E-14 to 7.3E-14
	(μmol m^2 d^{-1})	3.4 to 19.2	<0.1	2.5 to 44.4	1.6 to 4.1	0.6 to 1.3	0.9 to 1.1

Table S2: Fe, Mn, and Al concentrations in pore waters and sediments

Date	Station	Sample ID	Sample mid-depth (cm)	Sediment particles			Porewater	
				Fe (wt %)	Mn (ppm)	Al (wt%)	Fe (μmol kg^{-1})	Mn (μmol kg^{-1})
Feb. 2011	S1 (MC33)	AC1	0.5	3.25	635	4.77	3.0	2.421
		AC2	1.5	3.38	633	4.70	17.2	0.940
		AC3	2.5	3.31	647	4.78	110.1	0.546
		AC4	3.5	3.35	662	5.01	105.6	0.675
		AC5	4.5	3.22	649	4.65	93.5	0.520
		AC6	5.5	3.30	662	5.02	81.9	0.389
		AD1	7	-	-	-	52.6	0.271
		AD2	9	3.11	615	4.66	32.6	0.263
		AD3	11	-	-	-	27.3	0.304
		AD4	13	-	-	-	6.4	0.293
		AD5	15	3.09	612	4.69	2.5	0.209
		AD6	17	-	-	-	1.4	0.087
		AE1	19	-	-	-	0.8	0.040
		AE2	21	-	-	-	0.8	0.027
		AE3	23	-	-	-	0.7	0.028
		AE4	25	2.99	594	4.31	0.7	0.008
Feb. 2011	S2 (MC34)	AF1	0.5	3.58	627	4.77	1.5	0.585
		AF2	1.5	3.35	644	4.83	-	-
		AF3	2.5	3.24	649	4.74	1.1	0.399

		AF5	4.5	-	-	-	18.5	0.304
		AG1	6.5	3.32	672	4.94	11.1	0.264
		AG3	8.5	-	-	-	4.7	0.253
		AG5	10.5	3.24	647	4.85	14.5	0.285
		AH1	12.5	-	-	-	3.9	0.290
		AH3	14.5	3.02	595	4.32	3.8	0.285
		AH5	16.5	3.11	616	4.65	2.6	0.336
Feb. 2011	S3 (MC35)	AI1	0.5	3.43	627	4.49	1.6	0.597
		AI2	1.5	3.28	643	4.75	29.0	0.465
		AI3	2.5	3.24	642	4.75	91.1	0.373
		AI4	3.5	3.32	661	4.88	40.2	0.342
		AI5	4.5	-	-	-	37.1	0.262
		AI6	5.5	3.16	636	4.81	49.3	0.535
		AJ1	6.5	-	-	-	37.4	0.251
		AJ2	7.5	-	-	-	61.7	0.322
		AJ3	8.5	3.27	640	4.92	67.9	0.475
		AJ4	11.0	-	-	-	48.2	0.398
		AJ5	13.0	-	-	-	23.6	0.336
		AJ6	15.0	-	-	-	33.5	0.648
		AK1	17.0	3.00	593	4.57	3.8	0.181
		AK2	19.0	3.05	597	4.51	1.9	0.075
		AK3	21.0	-	-	-	1.6	0.005
		AK5	25.0	3.08	615	4.77	3.2	0.071
		AK6	27.0	-	-	-	2.9	0.052
		AL1	29.0	3.10	615	4.83	5.6	0.095

145

Supplementary Figures

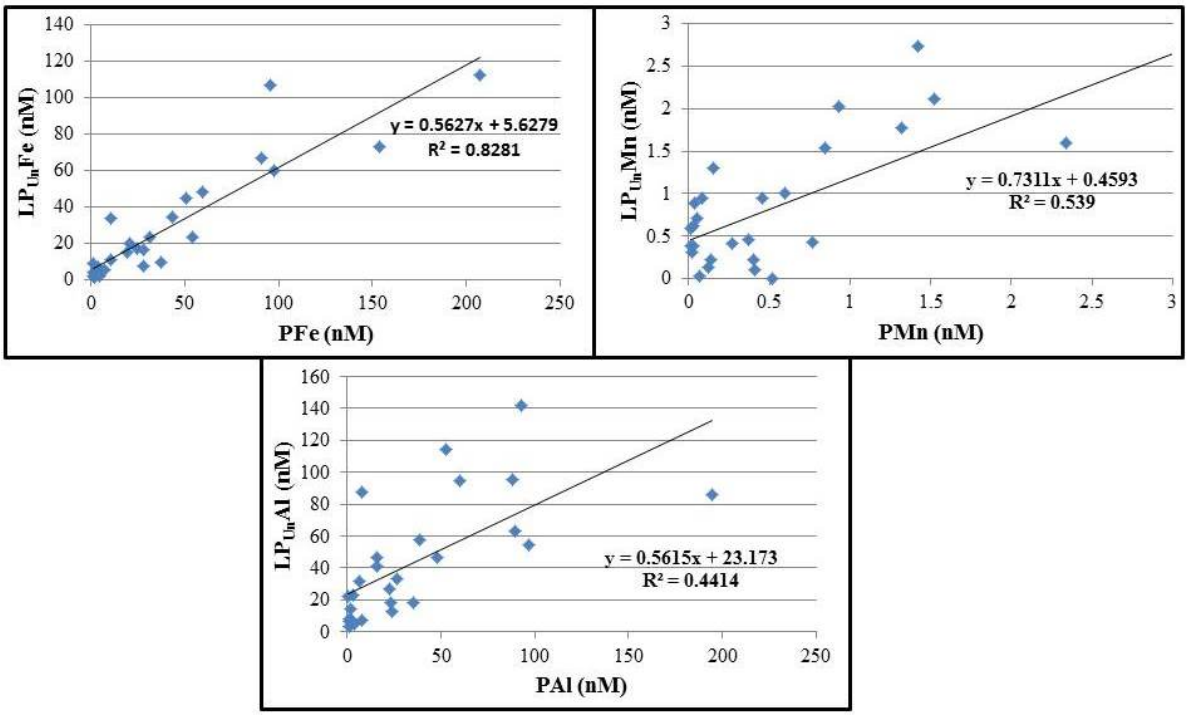

Figure S1: SAPS and OTE water sampler: Relationship of particulate trace metals from SAPS samplers (P) vs. leachable particulate trace metals from OTE water samplers (LP_{Un}). Data represents the entire data set collected at 20m, 50, and 100/150m.

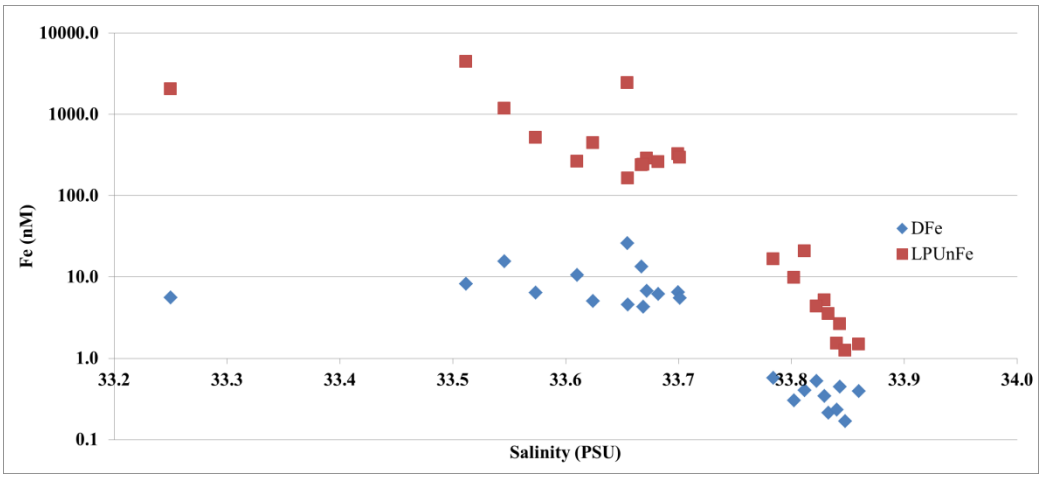

Figure S2: Tow-Fish surface samples: Relationship of salinity vs. dissolved (DFe) and leachable particulate Fe ($LP_{Un}Fe$) in surface waters. The Fe concentration along the y-axis is represented in a logarithmic scale. We applied a linear regression, to validate the relationship

between the DFe, $LP_{Un}Fe$ and salinity (not shown). With exception of the low salinity data point at 33.25 psu, the DFe and $LP_{Un}Fe$ vs. salinity data achieved an R^2 of 0.46 and 0.38, respectively.

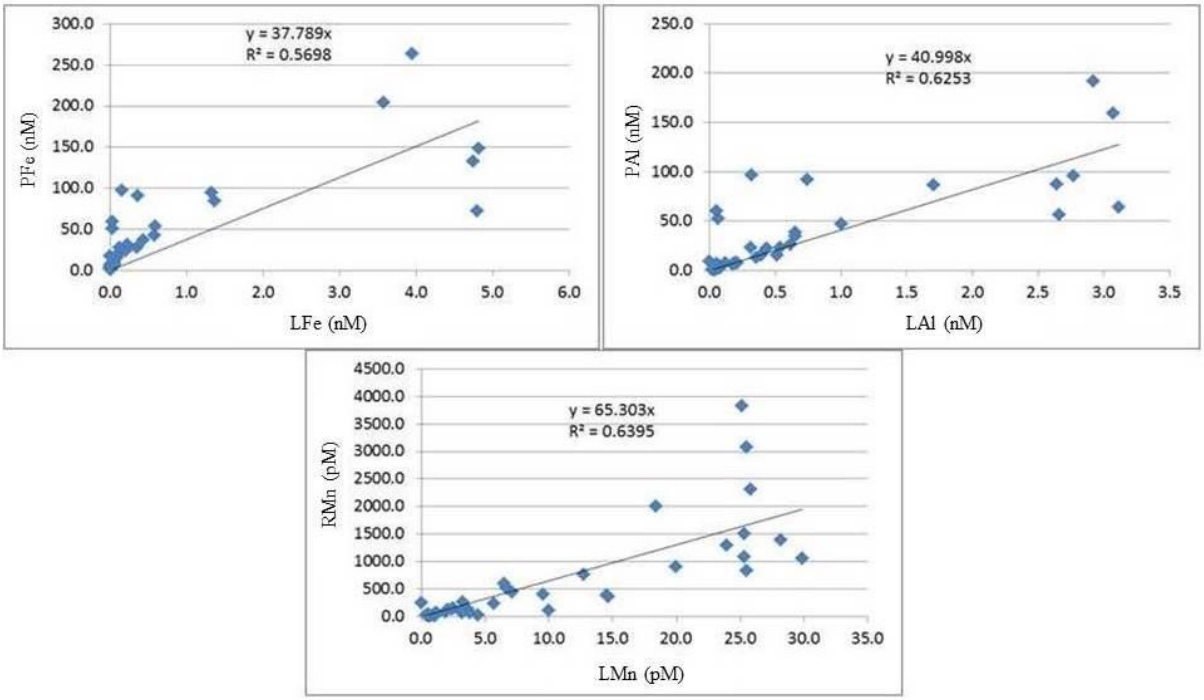

Figure S3: SAPS samples: Relationship between leachable (L) and refractory (R) Fe, Mn, and Al. Due to the high proportion of RP (98.9 – 99.2% for Fe) in the particulate fraction, using the particulate fraction, P, instead of R changes the linear regression with L just very little.

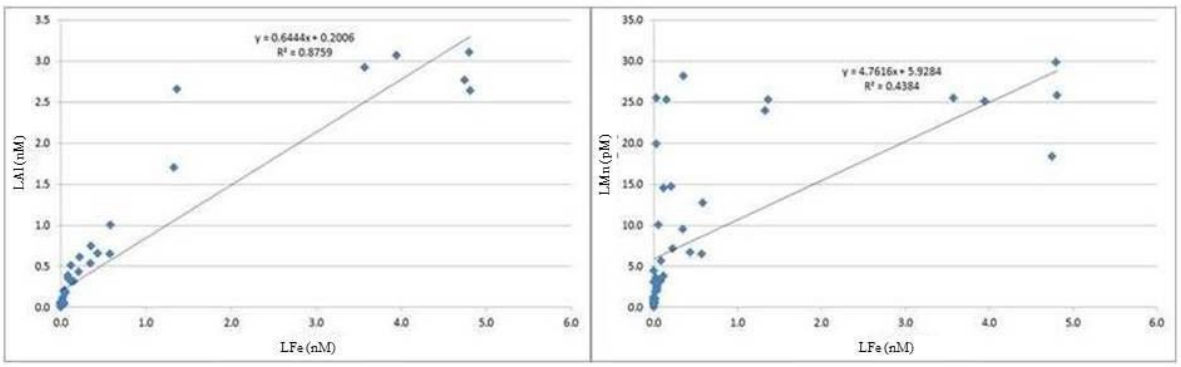

165

166 **Figure S4: SAPS samples:** Relationship between leachable Fe, Mn and Al.

167

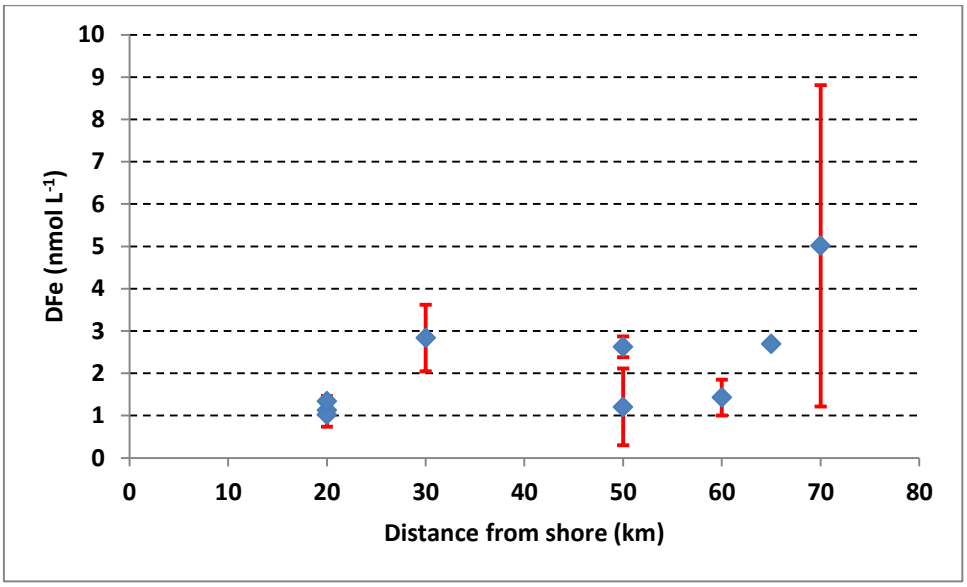

168

169 **Figure S5: OTE-water sampler:** Average dissolved Fe concentration between 100 and 400

170 m water depth versus distance to the coast line of South Georgia in kilometre.

References

Boudreux, B. P. and Scott, M. R.: A model for the diffusion-controlled growth of deep-sea manganese nodules, Americ. J. Sc., 278, 903-929, 1978.

de Jong, J., Schoemann, V., Lannuzel, D., Croot, P., de Baar, H. J. W., and Tison, J. L.: Natural iron fertilization of the Atlantic sector of the Southern Ocean by continental shelf sources of the Antarctic Peninsula, J. Geophys. Res., 117, 1-25, 2012.

Ho, T.-Y., Quigg, A., Finkel, Z. V., Milligan, A. J., Wyman, K., Falkowski, P. G., and Morel, F. M. M.: The elemental composition of some marine phytoplankton, J. Phycol., 39, 1145-1159, 2003.

Homoky, W. B., John, S. G., Conway, T. M., and Mills, R. A.: Distinct iron supply and isotope signatures from marine sediment dissolution, Nat. Commun., 4:2143, 2013.

Homoky, W. B., Severmann, S., McManus, J., Berelson, W. M., Riedel, T. E., Statham, P. J., and Mills, R. A.: Dissolved oxygen and suspended particles regulate the benthic flux of iron from continental margins, Mar. Chem., 134–135, 59-70, 2012.

John, S. G., Mendez, J., Moffett, J. W., and Adkins, J.: The flux of iron and iron isotopes from San Pedro Basin sediments, Geochim. Cosmochim. Act., 93, 14-29, 2012.

Kagaya, S., Maebe, E., Inoue, Y., Kamichatani, W., Kajiwara, T., Yanai, H., Saito, M., and Tohda, K.: A solid phase extraction using a chelate resin immobilizing carboxymethylated pentaethylenehexamine for separation and preconcentration of trace elements in water samples, Talanta, 79, 146-152, 2009.

Ma, S., Tao, Z., Yang, X., Yu, Y., Zhou, X., M, W., and Li, Z.: Estimation of marine primary productivity from satellite-derived phytoplankton absorption data, IEEE J-STARS, 7, 3084-3092, 2014.

McManus, J., Berelson, W. M., Severmann, S., Johnson, K. S., Hammond, D. E., Roy, M., and Coale, K. H.: Benthic manganese fluxes along the Oregon-California continental shelf and slope, Cont. Shelf Res., 43, 71-85, 2012.

Millero, F. J., Sotolongo, S., and Izaguirre, M.: The oxidation kinetics of Fe(II) in seawater, Geochim. Cosmochim. Act., 51, 793-801, 1987.

Raiswell, R. and Anderson, T. F.: Reactive iron enrichment in sediments deposited beneath euxinic bottom waters: constraints on supply by shelf recycling, Geological Society, London, Special Publications, 2005.

Rapp, I., Schlosser, C., Rusiecka, D., Gledhill, M., and Achterberg, E. P.: Automated preconcentration of Fe, Zn, Cu, Ni, Cd, Pb, Co, and Mn in seawater with analysis using high-resolution sector field inductively-coupled plasma mass spectrometry, Anal. Chimi. Acta, 976, 1-13, 2017.

Strzepek, R., Maldonado, M. T., Hunter, K. A., Frew, R. D., and Boyd, P. W.: Adaptive strategies by Southern Ocean phytoplankton to lessen iron limitation: Uptake of organically complexed iron and reduced cellular iron requirements, Limnol. Oceanogr., 56, 1983-2002, 2011.

Twining, B. S., Baines, S. B., Fisher, N. S., and Landry, M. R.: Cellular iron contents of plankton during the Southern Ocean Iron Experiment (SOFeX), Deep-Sea Res. I, 51, 1827-1850, 2004.